Progress In Electromagnetics Research M, Vol. 57, 25–34, 2017

Regional and Diurnal Variations of Rain Attenuation Obtained from Measurement of Raindrop Size Distribution over Indonesia at Ku, Ka and W Bands

Fadli Nauval[1], Marzuki[1, *], and Hiroyuki Hashiguchi[2]

Abstract—The measured raindrop size distribution (DSD) and the International Telecommunication Union Radiocommunication Sector (ITU-R) model have been used to elucidate the regional and diurnal variations of rain attenuation in Indonesia, for Ku-band (13.6 GHz), Ka-band (35.6 GHz), and W-band (96 GHz) frequencies. The DSDs were measured by the Parsivel disdrometer at Kototabang (KT; 100.32°E, 0.20°S), Padang (PD; 100.27°E, 0.54°S), Pontianak (PT; 109.37°E, 0.00°S), Manado (MN; 124.92°E, 1.55°N) and Biak (BK; 136.10°E, 1.18°S). In general, PD, KT and PT have lower rain attenuation than those at MN and BK, for the same rainfall rate, due to lower concentration of small-sized drops at these sites as reported by a previous study. Considerable differences between the attenuation obtained from the DSD and the ITU-R model are observed at all locations, in particular for very heavy rainfall ($R > 50$ mm/h). For $R < 50$ mm/h, the specific rain attenuation of measured DSD is in fairly good agreement with that obtained from the ITU-R model. The specific rain attenuation obtained from the DSD shows diurnal variation, in agreement with a previous study at KT. The diurnal variation of rain attenuation is dependent on the operating frequency and rainfall rate. At KT and PT, the lowest rain attenuation for Ku-band is observed during 06–12 LT, but during this period the largest attenuation is observed for Ka- and W-bands. These phenomena may be due to the increasing role of small and medium-sized drops by increasing frequency.

1. INTRODUCTION

The telecommunication system operating at frequencies above 5 GHz suffers from the rain attenuation due to the absorption and scattering of electromagnetic waves by rain particles. Rain attenuation reduces the link performance and availability of communication services. Therefore, it is the major issue for telecommunication system designers, particularly for high-frequency communication link design [1], and more especially in tropical regions which experience heavier rainfall intensities throughout the year [2].

The International Telecommunication Union Radiocommunication Sector (ITU-R) has provided a widely used method to predict the rain attenuation. The method requires only several inputs such as rainfall rate exceeded in time, the effective propagation path length, and the operating frequency. Despite its simplicity, some investigators have emphasized the inappropriateness of ITU-R method in tropical regions [3–7]. The tropical rainfall is different from that in the temperate region which is the main source of the ITU-R model. Tropical precipitation varies considerably across the region [8] and in a wide range of time-scales [2]. Moreover, the ITU-R model is based on T-matrix calculations and using oblate shaped drops and several model-based raindrop size distributions (DSDs) which are not necessarily representative of the real DSDs. Therefore, it is important to conduct more study on the characteristics of rain attenuation based on real DSDs particularly in the tropical region.

Received 5 March 2017, Accepted 22 April 2017, Scheduled 16 May 2017

* Corresponding author: Marzuki (marzuki@fmipa.unand.ac.id).

[1] Department of Physics, Andalas University, Padang, Indonesia. [2] Research Institute for Sustainable Humanosphere (RISH), Kyoto University, Japan.

In this article, the regional and diurnal variations of rain attenuation obtained from the measurement of DSD at five locations in Indonesia are investigated. In Indonesia, less work has been done to study the rain attenuation from the measured DSD. We have previously found that the specific rain attenuation shows diurnal variation with the largest attenuation observed in the morning hours because the raindrop spectrum of rain events in this period containing more small-sized drops [9]. However, the study is only based on the data collected from one location, i.e., at Kototabang, west Sumatra Indonesia. This paper is a follow-up of such previous study by analyzing the rain attenuation obtained from the measurement of DSD via a network of Parsivel disdrometers installed at Kototabang (KT), Padang (PD), Pontianak (PT), Manado (MN), and Biak (BK). The regional variation of DSD based on the data at these locations has been found [10]. The rain attenuation at Ku-band (13.6 GHz), Ka-band (35.6 GHz), and W-band (96 GHz) was estimated and compared with the ITU-R model [13]. These frequencies are used for the Global Precipitation Measurement/Dual-frequency Precipitation Radar (GPM/DPR) [14] and the Earth Clouds, Aerosols and Radiation Explorer (EarthCARE) cloud profiling radar [15].

2. DATA AND METHODOLOGY

The DSD was recorded by the OTT Parsivel. Table 1 summarizes the locations of each Parsivel and the observation period. Parsivel is a ground-based optical disdrometer which counts and measures simultaneously the fall speed and size of precipitation particles [10]. The DSD from this instrument was constructed for one-minute intervals, from 0.3 mm to 10 mm. Very light rain ($R < 0.1$ mm/h) was excluded in the analysis. To observe the diurnal variation of rain attenuation, the data were classified into four categories with 6-hour interval: 00–06, 06–12, 12–18, and 18–24 local time (LT). The diurnal variation of rain attenuation must be considered for the fade margin design [11]. The seasonal variation of DSD in Indonesia is not significant [12], so it is not considered in this study.

Table 1. Site parameters and observation periods for each location.

Site information	Period of disdrometer data
Kototabang (KT) 100.32°E, 0.20°S 865 m ASL	6 Jan., 2012–31 Jul., 2016 (1668 days)
Padang (PD) 100.27°E, 0.54°S 225 m ASL	31 Mar., 2014–26 Nov., 2016 (724 days)
Pontianak (PT) 109.37°E, 0.00°S 1 m ASL	6 Jan.–9 Sep. (236 days)
Manado (MN) 124.92°E, 1.55°N 92 m ASL	27 Feb.–7 Jun. (102 days)
Biak (BK) 136.10°E, 1.18°S 15 m ASL	11 Jan.–5 Jun. (147 days)

The specific rain attenuation in terms of the DSD was estimated by

$$A\,[\mathrm{dB/km}] = 4.343 \cdot 10^{-3} \int_0^\infty \sigma_{ext}(D, \lambda, m) N(D) dD. \tag{1}$$

where $N(D)$ ($m^{-3}\,\mathrm{mm}^{-1}$) is the DSD for the diameter of D (mm), ΔD the width of drop size class (mm), and σ_{ext} the Mie extinction cross section for water drops of diameter D which is in function of

wave length, drop size and complex refractive index. Parsivel employs nonuniform ΔD, increasing with increasing raindrop sizes that varies from 0.125 to 3 mm. The Mie extinction cross section of assumed spherical raindrops was deduced from [16, 17] for a temperature of 295 K. We used the value given by Liebe et al. [18] for m, the complex reflection coefficient of water droplets.

The specific rain attenuation coefficient is approximately related to rainfall rate (R) as

$$A\,[\mathrm{dB/km}] = aR^b, \tag{2}$$

where a and b are constants. The rainfall rate R (mm/h) was expressed in terms of the DSD as

$$R = 6\pi \cdot 10^{-4} \int_0^\infty D^3 v(D) N(D) dD, \tag{3}$$

where $v(D)$ is the raindrop fall speed in still air. Equation (2) was derived by the linear regression in logarithmic scale. The sequential intensity filtering technique (SIFT) was applied to reduce the effect of the spurious variability on disdrometric data [19].

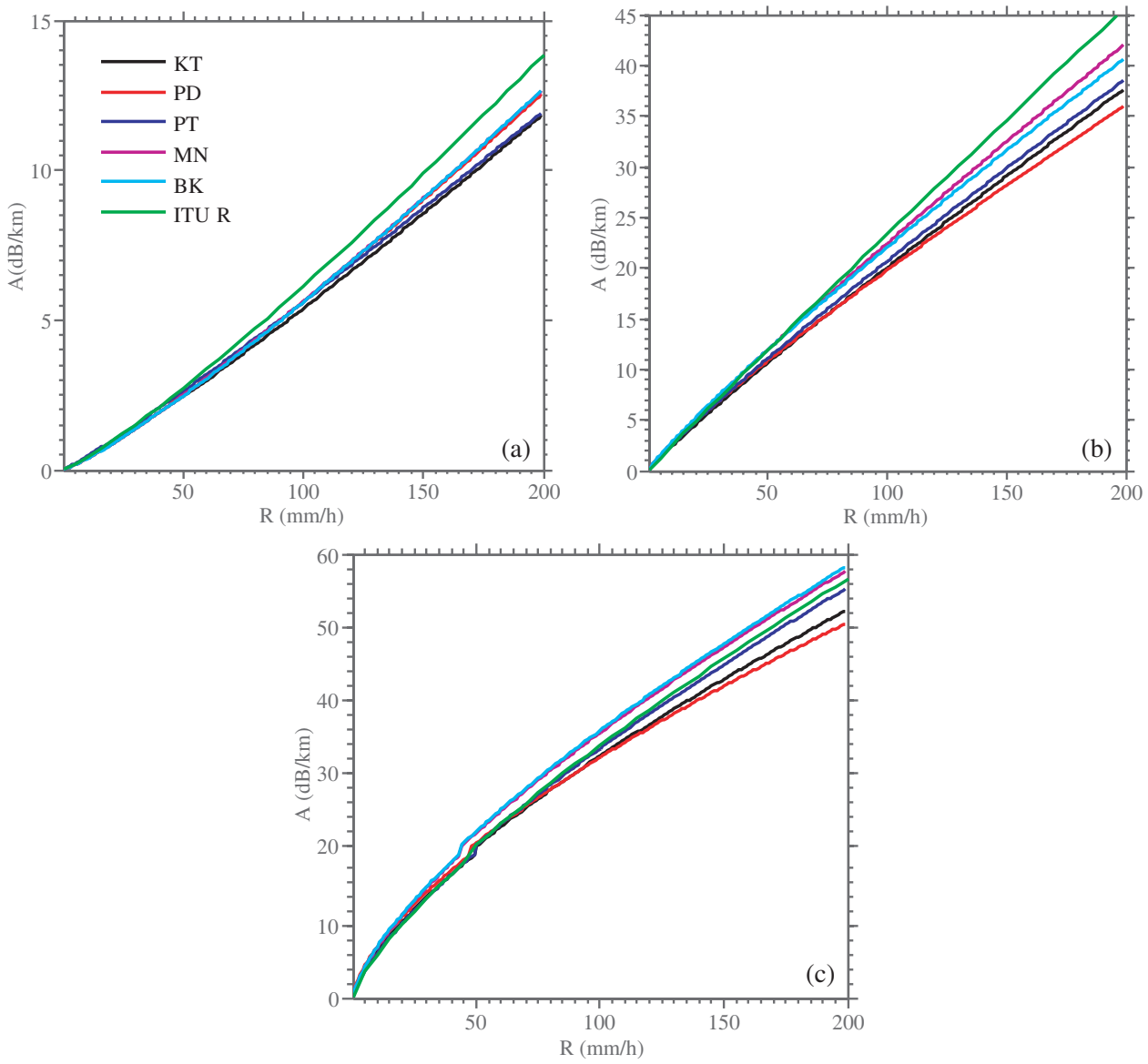

Figure 1. Specific rain attenuation obtained from the measured DSD on regional basis along with the ITU-R model [13]. KT, PD, PT, MN and BK indicate Kototabang, Padang, Pontianak, Manado and Biak, respectively. (a) Ku band. (b) Ka band. (c) W band.

3. RESULTS

3.1. Regional Variation of Rain Attenuation

Figure 1 shows a comparison of specific rain attenuation for the five locations along with the value estimated by the ITU-R model [13]. The power law equation of this figure is given in Table 2. The regional variations are more obvious with increasing frequency and rainfall rate. For the Ku-band frequency (Fig. 1(a)), the highest attenuation is observed at BK, followed by MN, particularly at very heavy rain. At rainfall rate (R) of 10, 50, 100 and 200 mm/h, the attenuation for BK (MN) are 0.37 (0.37), 2.46 (2.49), 5.60 (5.62) and 12.72 (12.70) dB/km, respectively. On the other hand, the lowest attenuation is observed at KT and PT where the values are 0.39 (0.44) 2.44 (2.62) 5.38 (5.60) 11.88 (11.97) dB/km, respectively, for the same rainfall rate. Thus, the difference between the highest and the lowest attenuation is not so significant for the Ku-band frequencies. Attenuation values at Ku-band frequencies for all locations are lower than the ITU-R model, especially for $R > 100$ mm/h. The specific rain attenuations from the ITU-R model at 10, 50, 100 and 200 mm/h are 0.41, 2.71, 6.13, 13.85 dB/km, correspondingly.

Table 2. Power law equation of specific rain attenuation versus rainfall rate for each location on diurnal basis.

	Ku-band				
Location	00–06 LT	06–12 LT	12–18 LT	18–24 LT	00–24 LT
KT	$A = 0.020R^{1.197}$	$A = 0.019R^{1.135}$	$A = 0.031R^{1.122}$	$A = 0.027R^{1.148}$	$A = 0.028R^{1.142}$
PD	$A = 0.015R^{1.294}$	$A = 0.018R^{1.248}$	$A = 0.029R^{1.141}$	$A = 0.026R^{1.170}$	$A = 0.026R^{1.167}$
PT	$A = 0.036R^{1.095}$	$A = 0.017R^{1.135}$	$A = 0.039R^{1.081}$	$A = 0.030R^{1.148}$	$A = 0.036R^{1.096}$
MN	$A = 0.020R^{1.220}$	$A = 0.022R^{1.203}$	$A = 0.027R^{1.165}$	$A = 0.025R^{1.165}$	$A = 0.025R^{1.176}$
BK	$A = 0.022R^{1.197}$	$A = 0.028R^{1.135}$	$A = 0.028R^{1.147}$	$A = 0.027R^{1.217}$	$A = 0.023R^{1.184}$
	Ka-band				
KT	$A = 0.281R^{0.926}$	$A = 0.237R^{1.005}$	$A = 0.305R^{0.908}$	$A = 0.297R^{0.915}$	$A = 0.298R^{0.914}$
PD	$A = 0.286R^{0.945}$	$A = 0.299R^{0.929}$	$A = 0.389R^{0.849}$	$A = 0.356R^{0.800}$	$A = 0.365R^{0.867}$
PT	$A = 0.343R^{0.893}$	$A = 0.231R^{1.031}$	$A = 0.286R^{0.979}$	$A = 0.356R^{0.800}$	$A = 0.325R^{0.902}$
MN	$A = 0.270R^{0.985}$	$A = 0.313R^{0.933}$	$A = 0.377R^{0.874}$	$A = 0.334R^{0.920}$	$A = 0.338R^{0.911}$
BK	$A = 0.407R^{0.859}$	$A = 0.263R^{0.994}$	$A = 0.295R^{0.949}$	$A = 0.253R^{1.006}$	$A = 0.371R^{0.887}$
	W-band				
KT	$A = 1.331R^{0.707}$	$A = 1.453R^{0.729}$	$A = 1.245R^{0.704}$	$A = 1.218R^{0.711}$	$A = 1.283R^{0.700}$
PD	$A = 1.766R^{0.652}$	$A = 1.770R^{0.649}$	$A = 1.439R^{0.670}$	$A = 1.412R^{0.670}$	$A = 1.548R^{0.658}$
PT	$A = 1.366R^{0.702}$	$A = 1.460R^{0.723}$	$A = 0.850R^{0.795}$	$A = 1.145R^{0.721}$	$A = 1.128R^{0.735}$
MN	$A = 1.230R^{0.758}$	$A = 1.268R^{0.724}$	$A = 1.415R^{0.624}$	$A = 1.456R^{0.700}$	$A = 1.366R^{0.707}$
BK	$A = 1.766R^{0.652}$	$A = 1.770R^{0.649}$	$A = 1.439R^{0.670}$	$A = 1.412R^{0.670}$	$A = 1.548R^{0.658}$

The difference between the specific rain attenuation estimated by the ITU-R model and that obtained from the DSD at Ka-band (Fig. 1(b)) is more significant than the Ku-band. The highest attenuation is observed at MN, and followed by BK, particularly for very heavy rains. For rainfall intensity of 10, 50, 100 and 200 mm/h the attenuation at MN (BK) are 2.75 (2.86) 11.93 (11.92) 22.43 (22.05) 42.18 (40.77) dB/km, respectively. Furthermore, the lowest specific attenuation is observed at PD and KT where the values are 2.68 (2.44) 10.85 (10.64) 19.78 (20.05) 36.08 (37.78) dB/km, accordingly. Like the Ku-band, the specific rain attenuation values for all locations at the Ka-band frequencies are also lower than the ITU-R model, in particular for $R \geq 100$ mm/h. For R of 10, 50, 100 and 200 mm/h, the ITU-R provides the values of 2.49, 11.09, 23.35, 45.78 dB/km. Thus, the difference between the specific rain attenuation estimated by the ITU-R model and that obtained from the DSD is approximately 3 dB/km, for the highest attenuation (MN) and is about 10 dB/km for the lowest

attenuation (PD), at rainfall rate of 200 mm/h.

For W-band (Fig. 1(c)), the specific rain attenuations at BK and MN are slightly larger than the ITU-R model. At R of 10, 50, 100 and 200 mm/h the attenuation at BK (MN) are 7.02 (6.96) 21.91 (21.71) 35.77 (35.44) 58.40 (57.85) dB/km, respectively. For the same intensity, the ITU-R provides

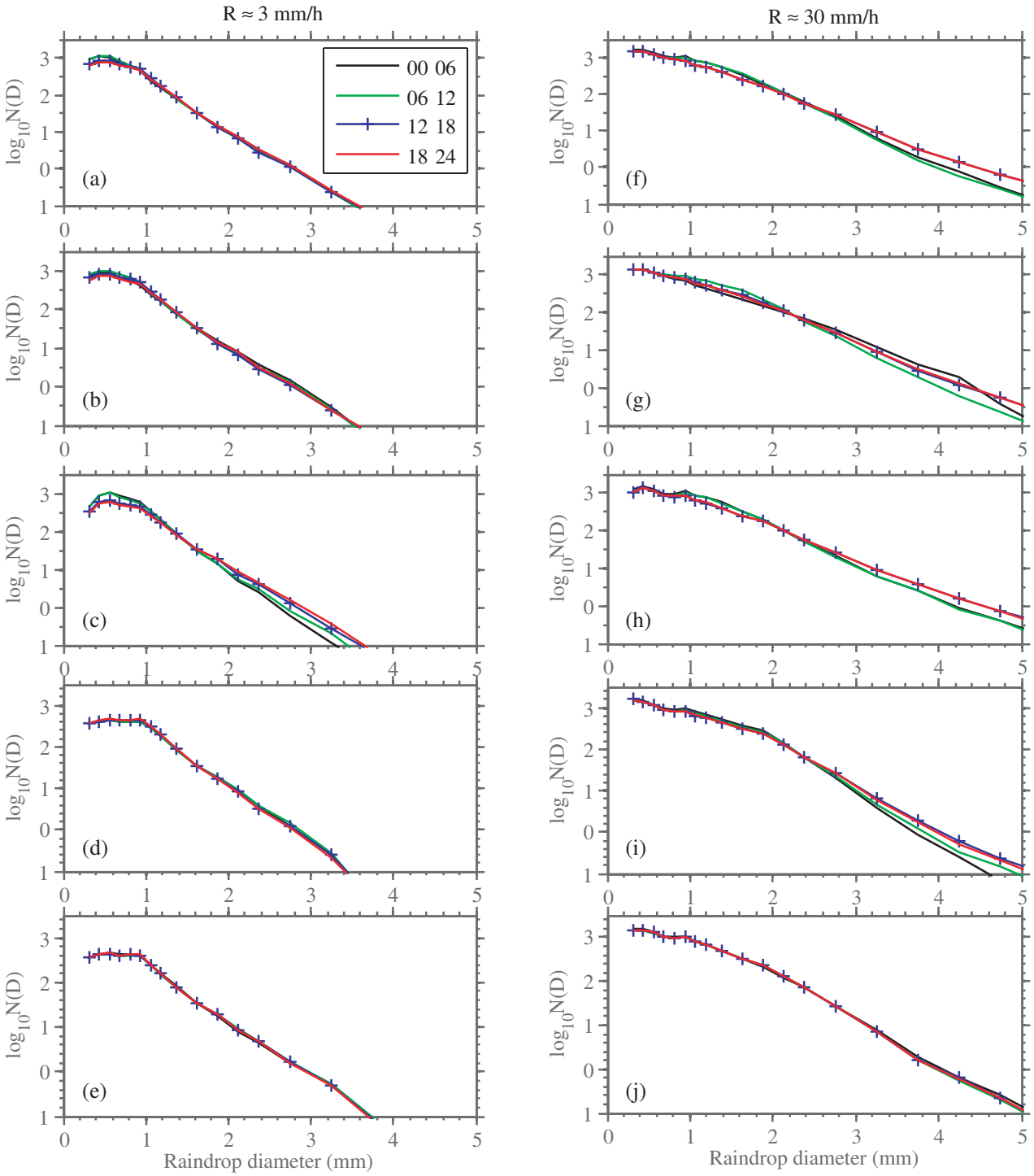

Figure 2. Averaged drop size distributions around 3 and 30 mm/h for each location on diurnal basis. (a) KT. (b) PD. (c) PT. (d) MN. (e) BK. (f) KT. (g) PD. (h) PT. (i) MN. (j) BK.

the values of 6.00, 20.03, 33.67, 56.59 dB/km. The lowest attenuation are observed at PD and KT where the values are 7.04 (6.43) 20.31 (19.83) 32.04 (32.22) 50.56 (52.35) dB/km, accordingly. Thus, the attenuation at BK is about 2 dB/km larger than the ITU-R model while the attenuation at PD is about 6 dB/km lower, at rainfall rate of 200 mm/h.

PD, KT and PT have a lower attenuation value than MN and BK, particularly for very heavy rains ($R > 50$ mm/h). This is consistent with the regional variation of the DSD as previously reported [10]. The DSDs at the three locations contain more large-size raindrops and less small-sized drop than MN and BK. At MN and BK,the DSDs have more small-sized raindrops. This condition is clearly

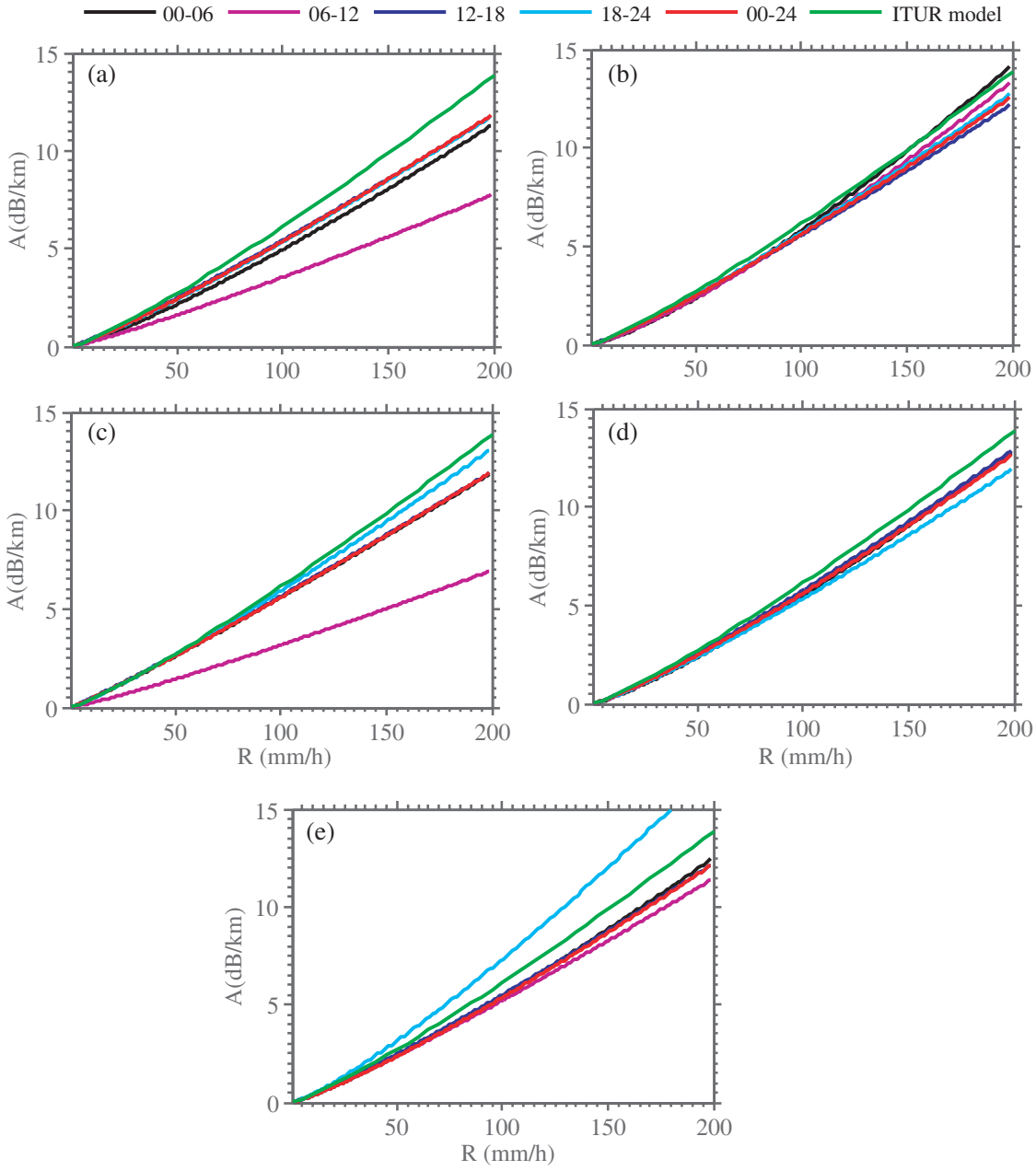

Figure 3. Specific rain attenuation obtained from the measured DSD on diurnal basis for Ku-band (13.6 GHz) along with the ITU-R model [13]. KT, PD, PT, MN and BK indicate Kototabang, Padang, Pontianak, Manado and Biak, respectively. (a) KT-Ku. (b) PD-Ku. (c) PT-Ku. (d) MN-Ku. (e) BK-Ku.

observed at very heavy rains. The role of small and medium-sized rain drops on specific attenuation is proportional to the increase of the rainfall intensity and operating frequency [9]. Therefore, the specific rain attenuation at MN and BK is higher than PD, KT and PT, particularly at very heavy rains.

3.2. Diurnal Variation of Rain Attenuation

To see the preliminary evidence of the diurnal variation of DSDs for each location, the DSDs for specific rain rate of 3 and 30 mm/h were averaged (Fig. 2). At light rain, a slight difference in the spectra could be seen at KT, PD and PT in which it had more small drops and less large-sized drops, during the first half of the day (00–12 LT). The evidence of diurnal variation of DSD becomes more obvious during heavy rain (Figs. 2(f)-(i)). The average spectra of KT, PD, and PT were much broader than MN and

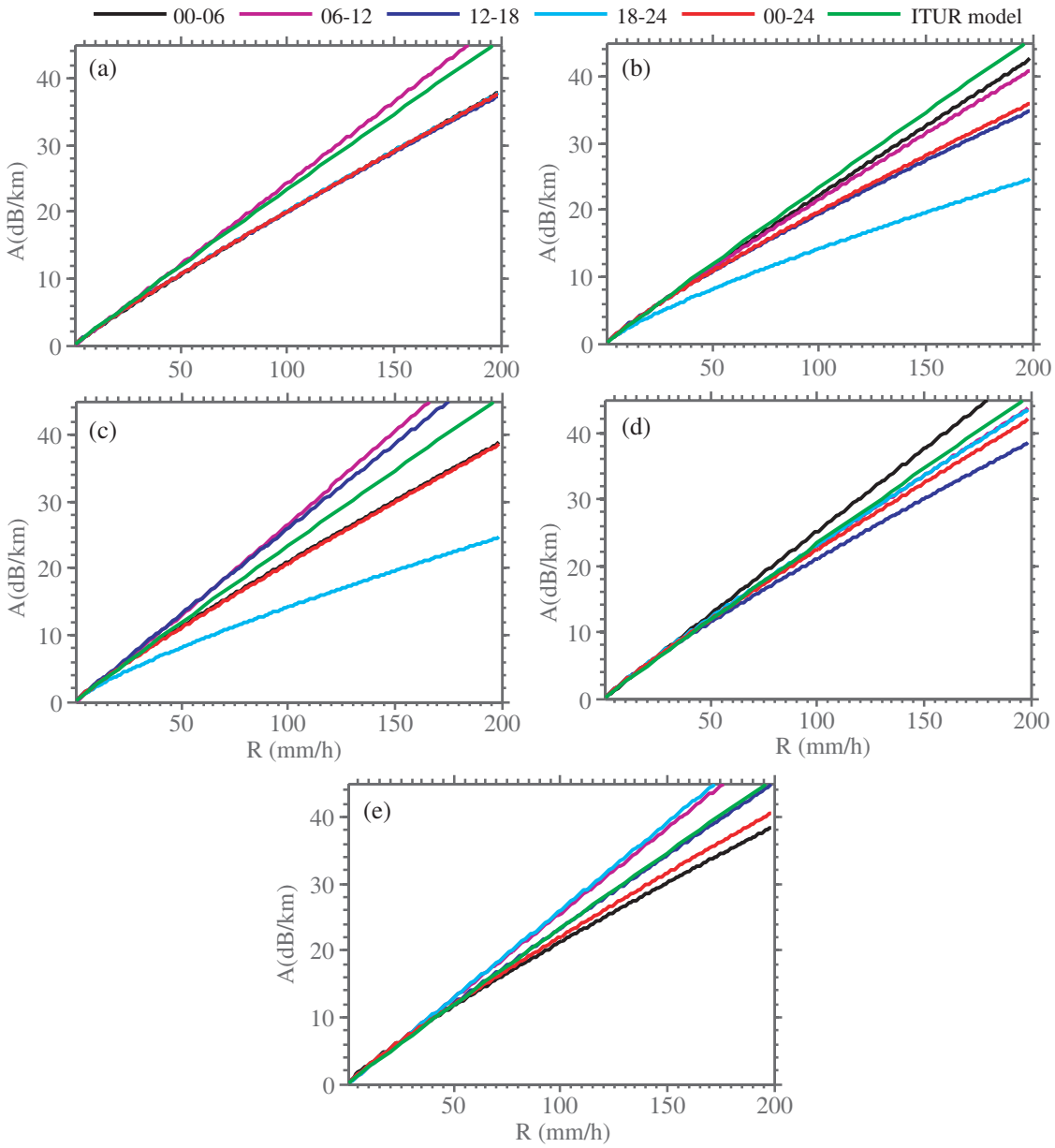

Figure 4. Same as Fig. 3, but for Ka-band (35.6 GHz). (a) KT-Ka. (b) PD-Ka. (c) PT-Ka. (d) MN-Ka. (e) BK-Ka.

BK, indicating that the spectra consists of more large-sized drops. Furthermore, the DSDs at KT, PD, PT and MN during the first half of the day have more small and medium-sized raindrops than during the second half of the day (12–24 LT).

Figure 3 shows the diurnal variation of specific rain attenuation for Ku-band along with the value estimated by the ITU-R model [13]. The power law equation of this figure is given in Table 2. In general, the ITU-R model overestimates the rain attenuation for all times, with the exception during 18–24 LT at BK. During this period the specific rain attenuation at BK is slightly larger than the ITU-R model. For example, at $R = 50$ and 100 mm/h the attenuations are 3.15 and 7.33 dB/km, respectively, in comparison with 2.71 and 6.13 mm/h from the ITU-R model. The diurnal variation of rain attenuation at PD and MN is not significant for Ku-band. The diurnal variation is more serious at KT and PT in which the rain attenuation during 06–12 LT is much smaller than other periods and the ITU-R model.

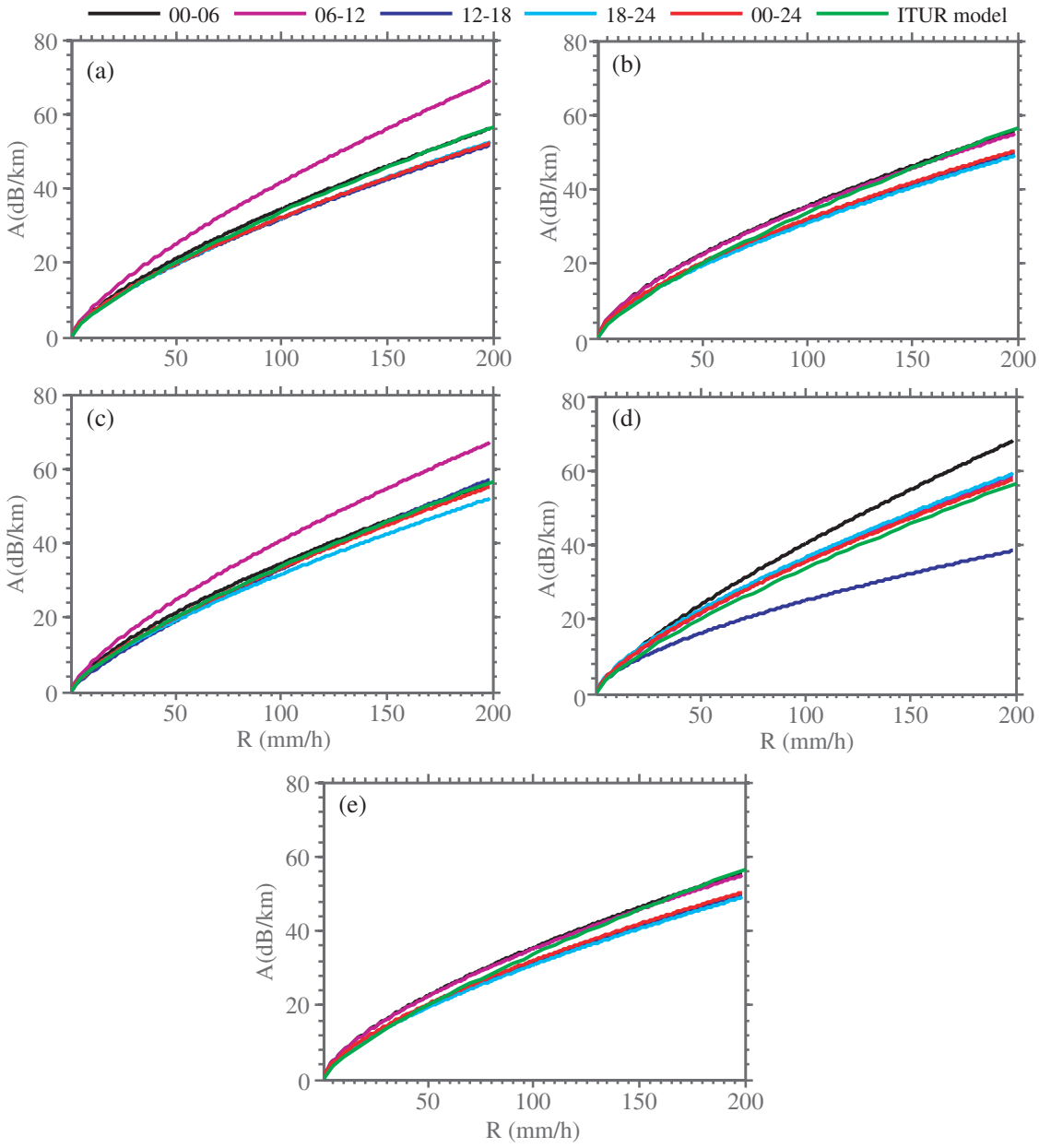

Figure 5. Same as Fig. 3, but for W-band (96 GHz). (a) KT-W. (b) PD-W. (c) PT-W. (d) MN-W. (e) BK-W.

At $R = 50$ and 100 mm/h the values for KT(PT) are 1.61 (1.44) and 3.54 (3.16) dB/km, respectively.

The diurnal variation of specific rain attenuation for the Ka-band is clearly visible at all locations (Fig. 4). At PD, the attenuation of all time periods are smaller than that predicted by the ITU-R models. However, at KT, PT, MN and BK, some periods have larger attenuations than that predicted by ITU-R models. At KT and PT, the attenuation during 06—12 LT is the highest value and is somewhat larger than the ITU-R model. The same characteristics is observed at BK. Moreover, at MN, the highest attenuation is observed during 00–06 LT and the difference between the highest and the lowest attenuation is not so significant.

For W-band frequency, the diurnal variations are significant at KT, PT and MN (Fig. 5). The highest attenuation at KT(PT) are observed during 06–12 LT with the value being 25.16 (24.70), 41.71 (67.29) dB/km for 50 and 100 mm/h, respectively. These values are much higher than that obtained by the ITU-R model, i.e., 20.03 and 33.67 dB/km. At MN, the highest attenuation values are observed during 00–06 LT. On the other hand, the lowest specific rain attenuation is observed during 12–18 LT. This is consistent with the characteristics of DSD given in Fig. 2. The specific rain attenuation is large during the period of DSD containing more small-sized raindrops, and vice versa.

4. CONCLUSIONS AND FUTURE WORKS

The result shows that the specific rain attenuation due to the tropical raindrops is strongly influenced by some variabilities. Such variabilities limit the accuracy of the ITU-R model. The specific rain attenuation found from the DSD measurement shows significant regional and diurnal variations. In general, the ITU-R model overestimates the attenuation for all examined locations, particularly for very heavy rains ($R > 50$ mm/h). PD, KT and PT have a lower attenuation than MN and BK. The regional variation of rain attenuation at rainfall rate smaller than 50 mm/h is relatively small and is in fairly good agreement with that obtained from the ITU-R model. The diurnal variation of rain attenuation is dependent on the frequency and rainfall rate. At KT and PT, the lowest rain attenuation for Ku-band is observed during 06–12 LT, but during this period the largest attenuation is observed for Ka and W-bands. This phenomena may be due to the increasing role of small and medium-sized drops being proportional to the increase of frequency. Thus, the variability of specific rain attenuation should be kept in mind when modeling the radio communication links in the tropical region such as for the fade margin design. The current result is from limited dataset, particularly at PT, MN and BK, more study with long data record must be done to apply the DSD variability into the ITU-R model. Furthermore, there are limitations with Parsivel instrument that may influence the current result. The instrument tends to underestimate the smallest raindrops, and overestimate the concentration of medium to large drops in the strong rainfall intensity. Therefore, the comparison of rain attenuation estimated from the Parsivel data with that obtained from other disdrometers such as 2D-Video Disdrometer will be conducted.

ACKNOWLEDGMENT

The Parsivel observation was partially funded by the Ministry of Education, Culture, Sports, Science and Technology of Japan (MEXT), as apart of the Japan Earth Observation System (EOS) Promotion Program (JEPP) under HARIMAU and SATREPS projects and Grants-in-Aids (23340142) of the Japan Society for the Promotion of Science (JSPS). The first author and co-authors were partially supported by the 2017 Student Creativity Program of Research (PKM-PE) and the 2017 International Joint Collaboration and Scientific Publication grants from the Ministry of Research, Technology and Higher Education of the Republic of Indonesia, respectively.

REFERENCES

1. Moupfouma, F. and L. Martin, "Modelling of the rainfall rate cumulative distribution for the design of satellite and terrestrial communication systems," *Int. J. Satellite Commun.*, Vol. 13, 105–115, 1995.

2. Marzuki, H. Hashiguchi, T. Shimomai, and W. L. Randeu, "Cumulative distributions of rainfall rate over Sumatra," *Progress In Electromagnetics Research M*, Vol. 49, 1–8, 2016.
3. Manabe, T., T. Ihara, J. Awaka, and Y. Furuhama, "The relationship of raindrop-size distribution to attenuation experiments at 50, 80, 140, and 240 GHz," *IEEE Trans. Antennas Propag.*, Vol. 35, 1326–1330, 1987.
4. Yeo, T. S., P. S. Kooi, M. S. Leong, and S. S. Ng, "Microwave attenuation due to rainfall at 21.225 GHz in the Singapore environment," *Electron. Lett.*, Vol. 26, No. 14, 1021–1022, 1990.
5. Yeo, T. S., P. S. Kooi, and M. S. Leong, "A two-year measurement of rainfall attenuation of CW microwaves in Singapore," *IEEE Trans. Antennas Propag.*, Vol. 41, No. 6, 709–712, 1993.
6. Zhou, Z. X., L. W. Li, T. S. Yeo, and M. S. Leong, "Analysis of experimental results on microwave propagation in Singapore's tropical rainfall environment," *Microwave Opt. Technol. Lett.*, Vol. 21, No. 6, 470–473, 1999.
7. Obiyemi, O. O., J. S. Ojo, and T. S. Ibiyemi, "Performance analysis of rain rate models for microwave propagation designs over tropical climate," *Progress In Electromagnetics Research M*, Vol. 39, 115–122, 2014, doi:10.2528/PIERM14083003.
8. Aldrian, E. and R. D. Susanto, "Identification of three dominant rainfall regions within Indonesia and their relationship to sea surface temperature," *Int. J. of Climatology*, Vol. 23, No. 12, 1435–1452, 2003.
9. Marzuki, T. Kozu, T. Shimomai, W. L. Randeu, H. Hashiguchi, and Y. Shibagaki, "Diurnal variation of rain attenuation obtained from measurement of raindrop size distribution in equatorial Indonesia," *IEEE Trans. Antennas Propag.*, Vol. 57, No. 4, 1191–1196, 2009.
10. Marzuki, H. Hashiguchi, M. K. Yamamoto, S. Mori, and M. D. Yamanaka, "Regional variability of raindrop size distribution over Indonesia," *Ann. Geophys.*, Vol. 31, 1941–1948, 2013, doi:10.5194/angeo-31-1941-2013.
11. Fiebig, U.-C. and C. Riva, "Impact of seasonal and diurnal variations on satellite system design in V band," *IEEE Trans. Antennas Propag.*, Vol. 52, No. 4, 923–932, 2004.
12. Kozu, T., K. K. Reddy, S. Mori, M. Thurai, J. T. Ong, D. N. Rao, and T. Shimomai, "Seasonal and diurnal variations of raindrop size distribution in Asian Monsoon Region," *J. Meteor. Soc. Japan. Ser. II*, Vol. 84A, 195–209, 2006.
13. Radiowave Propagation Series, I.T.U., "Specific attenuation model for rain for use in prediction methods," *Recommendation ITU-R P.838-3*, International Telecommunications Union, Geneva, 2005.
14. Hou, A. Y., R. K. Kakar, S. Neeck, A. A. Azarbarzin, C. D. Kummerow, M. Kojima, R. Oki, K. Nakamura, and T. Iguchi, "The global precipitation measurement mission," *Bull. Amer. Meteor. Soc.*, Vol. 95, 701–722, 2014, doi: 10.1175/BAMS-D-13-00164.1.
15. Illingworth, A. J., H. W. Barker, A. A. Beljaars, M. M. Ceccaldi, H. H. Chepfer, N. N. Clerbaux, J. J. Cole, J. J. Delano, C. C. Domenech, D. P. Donovan, S. S. Fukuda, M. M. Hirakata, R. J. Hogan, A. A. Huenerbein, P. P. Kollias, T. T. Kubota, T. T. Nakajima, T. Y. Nakajima, T. T. Nishizawa, Y. Y. Ohno, H. H. Okamoto, R. R. Oki, K. K. Sato, M. M. Satoh, M. W. Shephard, A. A. Velzquez-Blzquez, U. U. Wandinger, T. T. Wehr, and G. J. van Zadelhoff, "The EarthCARE satellite: The next step forward in global measurements of clouds, aerosols, precipitation, and radiation," *Bull. Amer. Meteor. Soc.*, Vol. 96, 1311–1332, 2015, doi: 10.1175/BAMS-D-12-00227.1.
16. Bohren, C. F. and D. R. Huffman, *Absorption and Scattering of Light by Small Particles*, John Wiley & Sons, Inc, 1983.
17. Mätzler, C., "MATLAB functions for Mie scattering and absorption Version 2," I*AP Research Report No. 2002-11*, Institut für angewandte Physik, Universität Bern, 2002.
18. Liebe, H. J., G. A. Hufford, and T. Manabe, "A model for the complex permittivity of water at frequencies below 1 THz", *Int. J. Infrared and Millimeter Waves*, Vol. 12, 659–674, 1991.
19. Lee, G. and I. Zawadzki, "Variability of drop size distributions: Noise and noise filtering in disdrometric data," *J. Applied Meteorology*, Vol. 44, 634–652, 2005.